ResearchGate

See discussions, stats, and author profiles for this publication at: https://www.researchgate.net/publication/229311662

Density evolution of absorption bandshapes in the water vapor OH-stretching fundamental and overtone: Evidence for molecular aggregation

ARTICLE *in* JOURNAL OF MOLECULAR STRUCTURE · MAY 2005

Impact Factor: 1.6 · DOI: 10.1016/j.molstruc.2004.12.060

CITATIONS
9

READS
21

4 AUTHORS, INCLUDING:

Andrei A. Vigasin
Russian Academy of Sciences
86 PUBLICATIONS **717** CITATIONS
SEE PROFILE

Yusuke Jin
National Institute of Advanced Industrial Sc…
51 PUBLICATIONS **287** CITATIONS
SEE PROFILE

Available from: Andrei A. Vigasin
Retrieved on: 24 January 2016

Available online at www.sciencedirect.com
SCIENCE DIRECT
Journal of Molecular Structure 742 (2005) 173–181
Journal of MOLECULAR STRUCTURE
www.elsevier.com/locate/molstruc

Density evolution of absorption bandshapes in the water vapor OH-stretching fundamental and overtone: evidence for molecular aggregation

A.A. Vigasin[a,*], A.I. Pavlyuchko[b], Y. Jin[c], S. Ikawa[c]

[a]*Wave Research Center, General Physics Institute, Russian Academy of Sciences, Vavilova 38, Moscow 119991, Russia*
[b]*Volgograd Technical University, Volgograd 400131, Russia*
[c]*Division of Chemistry, Graduate School of Science, Hokkaido University, Sapporo 060-0810, Japan*

Received 18 November 2004; revised 15 December 2004; accepted 26 December 2004
Available online 17 March 2005

Abstract

Hydrogen bonding among water molecules is largely responsible for non-ideality in water vapor. Spectroscopic observations in pressurized water vapor using either IR or Raman techniques provide evidence of substantial molecular aggregation up to the critical point and above. The mean size or the molar fractions of the individual aggregates which are formed are, however, very difficult to determine from the analysis of spectra. Present paper aims at the spectral bandshape modeling in sub-critical water vapor making use of available IR absorption spectra in the OH fundamental and overtone. The modeling is supported by quantum-chemical ab initio and anharmonic vibrational calculations for the water dimer, the results of which are compared with previous ab initio and low-temperature laboratory data.
© 2005 Elsevier B.V. All rights reserved.

Keywords: Water vapor; Water dimer; OH overtone; Anharmonic vibrational calculations

1. Introduction

Hydrogen bonding is known to give rise to pronounced frequency red-shift of the bonded OH oscillator accompanied by a significant increase in intensity of absorption. Very recently Kjaergaard et al. [1,2] have shown that ab initio calculations predict less IR molar intensity in the OH stretching first overtone in a dimer than in a monomer. In contrast to the OH fundamental no increase of the OH stretching overtone intensity happens upon hydrogen bonding. This result was then confirmed by Perchard and associates who have carried out a series of brilliant FTIR measurements in the OH fundamentals and overtones of the water dimers trapped in inert host matrices [3–5]. That the OH overtone molar intensity in a dimer is likely inferior to that of a monomer was recently suggested in [6] where Jin and Ikawa analyzed a series of FTIR absorption spectra of sub- and supercritical water vapor. This conclusion was drawn from examination of the temperature and pressure variations in the OH overtone integrated absorption intensity. Rational assumptions on the water dimer overtone intensity allowed Jin and Ikawa [6] to yield equilibrium constants characterizing the water dimer formation at temperature ranging from 623 to 673 K. Bondarenko and Gorbaty [7] have studied previously density variations of absorption in the water vapor OH fundamental. The enthalpy of dimerization was evaluated in [6,7] which is in reasonable agreement with independent data (see e.g. [8] where the dimerization enthalpy and entropy were evaluated from thermal conductivity data).

Extensive study of the IR absorption in pressurized water vapor has been undertaken in the early seventies by Vetrov et al. (see [9,10] and references therein) in the range of temperature and pressure from 26 to 500 °C and from 1 to 400 atm, respectively. The spectra were digitized at that time by hand and then stored in the form of a table with 20 to 100 cm^{-1} spacing among adjacent frequency readings. Hence, this unique set of data does no longer satisfy

* Corresponding author. Tel.: +7 095 952 02 26; fax: +7 095 952 05 40.
E-mail address: vigasin@kapella.gpi.ru (A.A. Vigasin).

0022-2860/$ - see front matter © 2005 Elsevier B.V. All rights reserved.
doi:10.1016/j.molstruc.2004.12.060

the standards of accuracy which are presently required from the infrared absorption spectra. In spite of this difficulty we enlisted a portion of spectra from [9] in order to be able to confront the dimer data retrieved from the overtone spectra with those obtained from the OH fundamental.

This paper explores the idea of a monomer–dimer equilibrium to simulate the IR absorption bandshapes density evolution in the regions of the OH fundamental and overtone. The monomer absorption was simulated in both spectral ranges by conventional line-by-line computations paying no account to possible line mixing effect, the role of which has to increase as individual monomer lines overlap at raising vapor density. In spite of substantial progress in laboratory characterization of the water dimer absorption, the knowledge of its vibrational spectrum is only fragmentary. Positions of all the four OH fundamentals in the vicinity of 3.3 μm are established nowadays with appreciable accuracy (see e.g. [11]). Neither the intensities of these bands nor the positions and intensities of the first overtone transitions are ever measured in the gas phase[1]. The only experimental data on these relate to the measurements for the dimers trapped in matrix environment (see [3–5] and references therein) though the extrapolation of matrix band origins and/or absorption intensities to those in the gas phase often requires an ill-determined correction. Ab initio quantum-chemical calculation is likely the only way to characterize the dimer potential energy and dipole surfaces in their totality. Being supplemented by anharmonic vibrational calculations this allows for making predictions for either fundamental or overtone vibrational band origins and their intensities.

To simulate absorption profiles in the OH-stretching fundamental the experimental positions of the vibrational bands along with their ab initio intensities were used in this paper. The dimer bands were suggested to have lorentzian bandshape with adjustable half-widths. The fractional abundance of dimers in a binary monomer–dimer mixture was found in the course of spectral fitting.

Our spectral fitting for the OH overtone returned positions, intensities and half-widths of three (effective) dimer bands in addition to the monomer mass fraction. Then the retrieved positions and intensities of the dimer overtone bands were compared with those obtained from the solution of an anharmonic vibrational problem based on the use of ab initio calculations of potential and dipole parameters for the water dimer.

The fractional abundance of monomers was thus found from the fitting of isothermal series of spectra taken at varying pressure. The retrieved monomer fractions from isothermal ‘fundamental’ and ‘overtone’ series were then imitated using mass-action law in order to evaluate the equilibrium constants for dimerization and to compare these with available literature data.

[1] Recent laboratory and open-air detection of the relatively high-lying water dimer overtone bands (see [12,13]) have to be pointed out, however.

2. Vibrational model

The modeling of the overtone spectra in the water dimer requires the solution of an anharmonic vibrational problem. We used variational anharmonic procedure, the details of which can be found elsewhere [14]. Briefly, the Hamiltonian was written in the form:

$$\hat{H}_{\mathrm{v}} = -\frac{\hbar^2}{2}\sum_{i,j}\frac{\partial}{\partial q_i}\left[\tau_{ij}(0) + \sum_k\left(\frac{\partial\tau_{ij}(q)}{\partial q_k}\right)_0 q_k + \frac{1}{2}\sum_{k,l}\left(\frac{\partial^2\tau_{ij}(q)}{\partial q_k\partial q_l}\right)_0 q_k q_l\right]\frac{\partial}{\partial q_j} + V(q).$$

Here $\tau_{ij}(q)$ are the elements of the kinematic matrix and $V(q)$ is the potential energy function. The latter was assumed in terms of Morse functions for OH-stretching coordinates and the fourth order polynomials for intermolecular stretch and bending vibrations:

$$V(q) = \frac{1}{2}\sum_{i,j}D_{ij}x_ix_j + \frac{1}{6}\sum_{i,j,k}D_{ijk}x_ix_jx_k + \frac{1}{24}\sum_{i,j,k,l}D_{ijkl}x_ix_jx_kx_l. \quad (1)$$

Here

$$x_i = \begin{cases} 1 - \mathrm{e}^{-\alpha_i r_i} & \text{for OH stretches,} \\ q_i & \text{for all other coordinates,} \end{cases}$$

q stands for dimensionless coordinates. Table 1 lists the potential parameters in Eq. (1) which were used in our calculations for the water monomer and dimer. These parameters have been determined in the course of solution of inverse spectroscopic problem for the monomer vibrational transitions up to ca. 11,000 cm^{-1} (see Table 2) and the water dimer fundamentals in the OH-stretching range (see Table 3).

To calculate matrix elements

$$H_{kn,ml} = \langle\chi_{kn}|\hat{H}_{\mathrm{v}}|\chi_{ml}\rangle$$

the variational functions χ_{kn} were used in the form of a product

$$\chi_{\mathrm{kn}} = \prod_i \phi_{k_i}(r_{\mathrm{i}})\prod_s \psi_{n_{\mathrm{s}}}(Q_{\mathrm{s}})$$

of the Morse oscillator $\phi_{k_i}(r_i)$ and harmonic oscillator $\psi_{n_{\mathrm{s}}}(Q_{\mathrm{s}})$ wave functions. Curvilinear coordinates Q_{s} were introduced in terms of a linear combination of valence coordinates which diagonalize the relevant harmonic part of the total vibrational Hamiltonian.

Table 1
Potential function for H_2O monomer and dimer

Monomer		Dimer			
		PA		PD	
α_r	2.15	α_r	2.15	α_{r_f}	2.15
				α_{r_b}	2.15
D_{rr}	1.8313	D_{rr}	1.8291	$D_{r_f r_f}$	1.8404
				$D_{r_b r_b}$	1.7565
$D_{rr'}$	−0.0205	$D_{rr'}$	−0.0155	$D_{r_f r_b}$	−0.0205
$D_{r\varphi}$	0.1197	$D_{r\varphi_a}$	0.1197	$D_{r_f\varphi_d}$	0.1197
				$D_{r_b\varphi_d}$	0.1197
$D_{\varphi\varphi}$	0.7025	$D_{\varphi_a\varphi_a}$	0.6764	$D_{\varphi_d\varphi_d}$	0.6774
$D_{rr\varphi}$	0.1586	$D_{rr\varphi_a}$	0.1586	$D_{r_f r_f\varphi_d}$	0.1586
				$D_{r_b r_b\varphi_d}$	0.1586
$D_{r\varphi\varphi}$	−0.3259	$D_{r\varphi_a\varphi_a}$	−0.3259	$D_{r_f\varphi_d\varphi_d}$	−0.3259
				$D_{r_b\varphi_d\varphi_d}$	−0.3259
$D_{\varphi\varphi\varphi}$	−0.8330	$D_{\varphi_a\varphi_a\varphi_a}$	−0.8330	$D_{\varphi_d\varphi_d\varphi_d}$	−0.8330
$D_{\varphi\varphi\varphi\varphi}$	−0.3192	$D_{\varphi_a\varphi_a\varphi_a\varphi_a}$	−0.3192	$D_{\varphi_d\varphi_d\varphi_d\varphi_d}$	−0.3192

PA and PD means hereafter proton acceptor and proton donor molecules, respectively; r stands for the OH stretching coordinate in a monomer or for those in the PA molecule in a dimer; r_f and r_b refer to 'free' and 'bonded' OH bonds in a PD molecule, respectively; φ, φ_a, and φ_d stand for bending coordinates in a monomer, PA, and PD molecules, respectively. The relevant units are: [α] = Å^{-1}, [D] = mdyn·Å, [r] = Å, [φ] = radians.

Basis wave functions appropriate to intramolecular vibrations have been used in the calculations for the water dimer. In all cases the achievement of the variational threshold was checked for the computed eigenvalues.

The intensities of vibrational transitions were calculated employing the first and the second dipole derivatives with respect to valence coordinates

$$\frac{\partial\vec{\mu}}{\partial q_i} = \frac{\vec{\mu}_+ - \vec{\mu}_-}{\Delta q_i},$$

$$\frac{\partial^2\vec{\mu}}{\partial q_i^2} = \frac{\vec{\mu}_+ + \vec{\mu}_- - 2\vec{\mu}_0}{\Delta q_i^2},$$

$$\frac{\partial^2\vec{\mu}}{\partial q_i\partial q_j} = \frac{\vec{\mu}_{++} + \vec{\mu}_{--} - \vec{\mu}_{+-} - \vec{\mu}_{-+}}{4\Delta q_i\Delta q_j}. \quad (i \neq j)$$

Here $\vec{\mu}_0$ means the dipole moment relevant to equilibrium configuration, $\vec{\mu}_+$ and $\vec{\mu}_-$ stand for the dipole moment changed following the increase (decrease) of a valence coordinate q_i by the step Δq_i. Analogously, $\vec{\mu}_{++}$, $\vec{\mu}_{--}$, $\vec{\mu}_{+-}$, $\vec{\mu}_{-+}$ relate to simultaneous change in q_i and q_j coordinates by steps Δq_i and Δq_j. The above dipole moments were calculated ab initio using GAMESS [15] package for the molecules, the geometry of which was distorted accordingly with respect to that at equilibrium. Curvilinear relationship between valence and Carthesian coordinates has been accounted for. The adopted step Δq_i was set to 0.01 Å for stretching and 0.01 radians for bending coordinates, respectively.

Table 2
Frequencies ν(cm^{-1}) and intensities I (10^{-8} cm^2 mol^{-1} s^{-1}) of the H_2O monomer

HITRAN database [16]		This work ab initio based variational calcs[a]	
ν	I	ν	I
1594.6	31.75	1594.4	29.72
3151.6	0.2271	3152.0	0.1667
3657.1	1.486	3658.6	1.362
3755.9	21.6	3755.3	19.44
4666.8	0.0012	4669.6	0.0039
5235.0	0.1115	5232.6	0.1119
5331.3	2.416	5332.9	1.512
6775.0	0.0074	6770.6	0.0038
6871.7	0.1142	6875.0	0.0009
7201.5	0.1836	7203.2	0.1378
7249.8	1.69	7247.9	1.107
7445.1	0.0110	7446.5	0.0537
8761.5	0.0044	8759.8	0.0056
8807.1	0.1058	8807.6	0.0798
9000.1	0.0022	9006.8	0
10599.7	0.0063	10594.1	0.0051
10613.0	0.0511	10605.4	0.0659
10868.8	0.0017	10875.3	0.0025
11032.4	0.0057	11032.8	0.0012

[a] Dipole moment function was obtained at MP2/6-311G(2d,2p) level of quantum-chemical calculations.

Table 3
Measured and calculated frequencies and relative intensities of OH-stretching vibrations in $(H_2O)_2$ dimer

	Experimental		Ab initio				
	Gas phase	Ne matrix [5]	[17]	[18]	[19]	[2]	This work[a]
ν_3 (PA)	3745.48	3750	3917	4123	3713	3745	3745
I_{rel}	n/a	n/a	50.5	46.3	43.5	27.0	26.5
ν_1 (PA)	3660	3660.5	3799	3989	3626	3656	3660
I_{rel}	n/a	2.7	5.25	2.7	14.3	5.0	5.9
ν_3 (PD)	3735	3733.7	3907	4088	3679	3730	3735
I_{rel}	n/a	47	40.4	39	40.7	35	42
ν_1 (PD)	3601	3590.5	3758	3873	3548	3598	3601
I_{rel}	n/a	100	100	100	100	100	100
(I_{abs})	n/a	n/a	(99.5)	(141)	(90.7)	(130.8)	(104.2)

The relative intensities are scaled to a ν_1 (PD) intensity of 100 appropriate to each individual intensity data set. Absolute intensities of ν_1 (PD) in 10^{-8} cm^2 mol^{-1} s^{-1} are given in parentheses in the bottom line.

[a] Vibrational frequencies are obtained using potential parameteres listed in Table 1. Intensities are calculated using ab initio dipole parameters as described in Section 2.

Table 2 demonstrates good agreement between our calculated H_2O monomer frequencies and intensities and the data taken from the HITRAN database [16]. Note, however, that the difference in intensity is significant in some cases especially for weak transitions.

Table 3 shows the intensity variations among OH stretching vibrations in a dimer according to different sources. On the average ab initio calculations of the relative intensities prove to nicely fit the observations in the OH fundamental range for the matrix trapped water dimers.

The data in the rightmost column of the Table 3 which refer to ab initio calculations of our own at 6-311 G(2d,2p)/MP2 level, have been adopted in our forthcoming simulation of the spectral profile.

3. Experimental

Salient features of the high-density IR experiments can be found elsewhere [6,9,10]. Briefly, the experiments by Vetrov et al. [9,10] were carried out using medium-resolution (7 cm^{-1}) UR-20 spectrophotometer equipped with diagram tape logging. The spectra were recorded at ~200 fixed pressure-temperature parameters on a grid extending from 1 to 400 atm and from 299 to 773 K, respectively.

Recent experiments by Jin and Ikawa [6] were made using Perkin–Elmer 2000 Fourier-transform spectrometer operating at 2 cm^{-1} spectral resolution. The pressure–temperature range in which the spectra were recorded, covered intervals from 20 to 400 bars and from 373 to 673 K, respectively.

Fig. 1 shows approximately the domain of ρPT parameters (diagram of states is taken from the NIST Chemistry WebBook [20]) for which the IR absorption spectra either in the overtone or in the fundamental were selected for our spectral fit.

4. Spectral fit

Molecular association is expected to start from the formation of dimers. Hence, the spectral absorption coefficient can be represented in terms of monomer plus dimer contributions (see e.g. [21]):

$$\kappa(\nu) = \frac{N_0 \rho L}{\mu_{\mathrm{mon}}} \left(\sigma_{\mathrm{mon}}(\nu) + \frac{\alpha_{\mathrm{dim}}}{2} (\sigma_{\mathrm{dim}}(\nu) - 2\sigma_{\mathrm{mon}}(\nu)) \right). \quad (2)$$

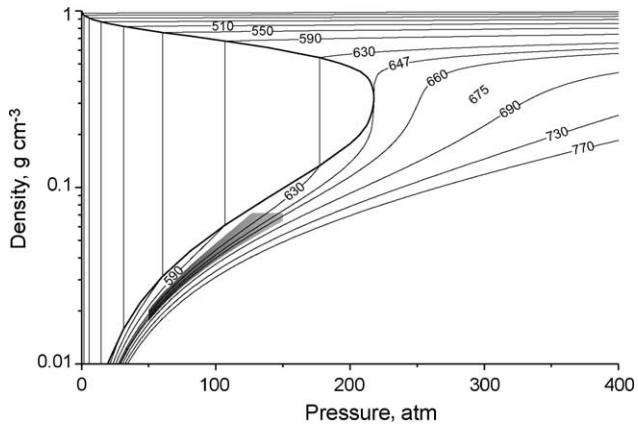

Fig. 1. Diagram of states for water. Shaded area shows the range of ρPT parameters for which the IR spectra were analyzed.

Here N_0 is the Avagadro's number, ρ is density, μ_{mon} is the monomer molecular mass, L stands for the optical path, α_{dim} is the water dimer mass fraction, $\sigma_{\mathrm{mon}}(\nu)$ and $\sigma_{\mathrm{dim}}(\nu)$ are the monomer and dimer absorption cross-sections, respectively. In all cases the observed spectral profiles are nicely reproduced using Eq. (2) as it is shown below, though the assumption of a binary mixture obviously fails at pressure as high as ca. 100 atm.

4.1. OH-stretching fundamental

The spectra obtained by Vetrov et al. [9,10] were used in the form of the wave number-absorption cross-section table with 20 cm^{-1} spacing between adjacent frequency readings. Systematic errors both in frequency calibration and in absorption intensity are likely to be hidden in these spectra. The amount of these errors is presently difficult to evaluate. Originally the systematic error of the spectral absorption coefficient was bracketed in the range from 8 to 12% in the vicinity of the maxima of absorption. The quality of these spectra is good enough, however, to clearly demonstrate the tendency in the spectral bandshape variations at elevated water vapor density, in particular, the pronounced red-shift of the band center accompanied by dramatic increase in the integrated intensity of a band. This evolution was interpreted in [9,10] in terms of unequivocal manifestation of molecular aggregation in steam.

Following this concept we suggested that the water dimers are largely responsible for the spectral bandshape transformations which take place as the density of steam starts to increase. The spectra of the monomeric constituent in a mixture can be modeled by virtue of line-by-line calculations using the HITRAN database [16]. Unfortunately, the self-broadening coefficients for the water vapor OH-fundamental are unavailable from the HITRAN version [16][2]. For a selection of water vapor lines these have been measured very recently by Zou and Varanasi [22]. The spectral range of our interest extends, however, beyond the interval for which Zou and Varanasi reported their accurate data. That is why the band averaged self-broadening half-widths in the form γ [cm^{-1} atm^{-1}] = $0.41 \times (296/T)^{0.7}$ were roughly admitted. Both the multiplier and the exponent in the above expression roughly correspond to those parameters averaged over the linelist reported by Zou and Varanasi [22]. No line-mixing effect was taken into account though this may represent a problem especially at elevated densities.

The accurate positions of three OH-stretching dimer fundamentals are known from high resolution spectroscopic probes in molecular beams. The only exception is a presumably low intense symmetrical acceptor stretch

[2] The available self-broadening and shifting parameters apply to relatively low-density vapor only, their use for dense media has to be considered as unavoidable compromise.

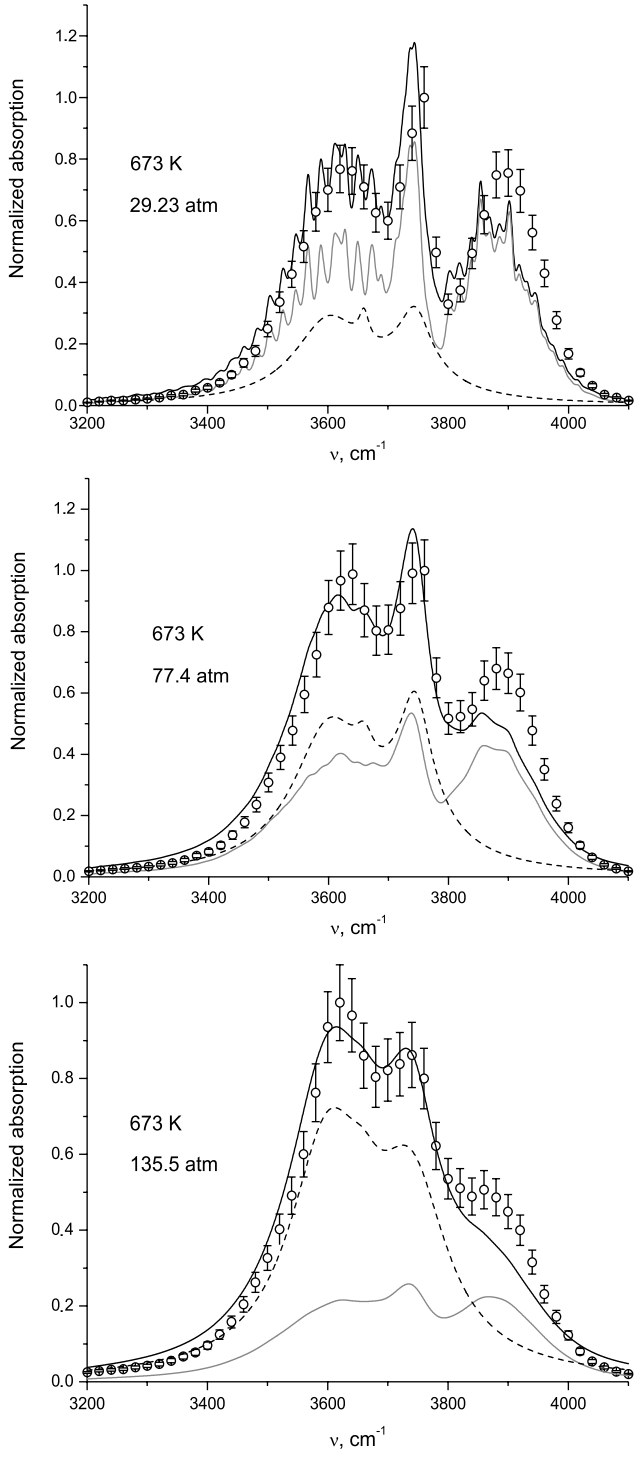

Fig. 2. Water vapor absorption in the OH stretching fundamental. Points with error bars stand for experimental data from [9]. Light, dash, and solid traces refer to the monomer, dimer, and resulting spectral profiles, respectively.

which was positioned in [23] using available data on the dimer bands taken from matrix isolation experiments. The ab initio calculated vibrational origins for the OH-stretching fundamentals were totally ignored so that the experimental gas phase vibrational frequencies were adopted. The intensities for these four bands were taken from our ab initio calculations as shown in the rightmost column of Table 3. Presupposing a binary monomer–dimer mixture, the only unknown parameters are therefore the dimer band shapes and the fractional abundance of dimers (monomers) in a mixture. Since the dimer rotational constants are significantly smaller than those in a monomer, the expected dimer bands should be much narrower and more symmetrical than the monomer bands. One has to admit, however, that inhomogeneous broadening can give rise to much larger dimer features than might be expected for rigid dimers. The dimer bands were assumed in our simulation to have a lorentzian shape with adjustable bandwidths. The latter were subject to independent variations in the course of spectral fitting.

Overall 50 spectra from [9] were simulated along four isotherms: 598, 623, 653, and 673 K. In all cases the quality of the spectral fit was surprisingly good. Typical examples of the fitted spectra are shown in Fig. 2. Interestingly, the quality of a fit looks by eye even better at higher densities than at lower ones, notwithstanding the expectation of higher water oligomers formation at densities at which the extent of dimerization approaches a dozen of percents. This can be understood in terms of a similarity among spectral features which characterize small water aggregates of different size. Intramolecular vibrations in any of the water oligomers comprise stretches of free and H-bonded OH bonds. Each H_2O unit in the aggregates from trimer to pentamer has one OH bond free and one hydrogen bonded OH bond.

Pressure variations of the monomer mass fraction along the 673 K isotherm are shown in Fig. 3. The only portion of this dependence which complies with dimers formation lies obviously inferior to an inflection point, since in a binary mixture the second derivative of $\partial^2\alpha_{mon}/\partial P^2$ at $T=$const does not change its sign as a function of pressure.

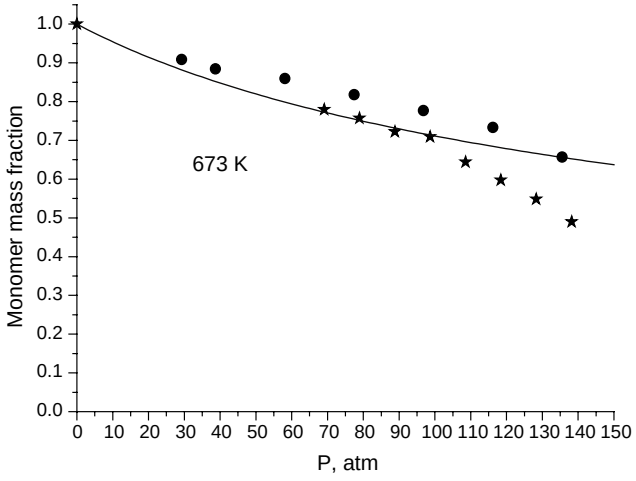

Fig. 3. Pressure variations of the water monomer mass fraction along the 673 K isotherm. The circles and asterisks refer to the values obtained from the spectral fit in the fundamental and overtone ranges, respectively.

Table 4
Equilibrium constants K_p retrieved from the spectral fit in the fundamental and overtone OH-stretching ranges

T (K)	K_p (atm^{-1})	
	Fundamental	Overtone
598	0.00228	–
623	0.00229	–
650	–	0.0025
653	0.00173	–
673	0.0017	0.0024

This makes it possible to evaluate the equilibrium constants shown in Table 4. It is noteworthy that the assumption of the dominant dimer formation fails roughly at pressure P exceeding ca. 100 atm that is when the dimer mass fraction gets higher than about 20–30%.

4.2. OH overtone

The water monomer absorption in the first OH-stretching overtone can be simulated using complete set of rovibrational line parameters compiled in the HITRAN database [16]. Note that the HITRAN line-by-line integrated absorption intensity (reduced to 673 K) for an isolated monomer in the frequency range from 6200 to 7800 cm^{-1} equals 4.0 km mol^{-1}. We shall comment on this figure below in due course.

The absorption features attributable to the water dimer in the OH first overtone are only known from the matrix isolation data. The more reliable of these have been reported recently by Perchard et al. [3–5] from the measurements in Ar, N_2, and Ne matrices. An extension of matrix data to the gas phase meets usually a difficulty since for instance, in an Ar matrix the water molecules are known to rotate freely, whereas in a nitrogen matrix the dimer vibrational levels are notably perturbed by the nitrogen molecule quadrupole. Of the matrices listed above the Neon matrix, however, is the weakest perturber. Table 5 shows good correspondence between the Ne matrix data for the water dimer and ab initio calculations.

The expected number of individual dimer vibrational bands in the overtone region is largely in excess of that in the fundamental range. Therefore, instead of using a few tens of adjustable parameters we restricted ourselves by introducing effective dimer overtone bands. Three effective dimer bands were suggested, whose positions, intensity and bandwidths are subject to the search in the course of fitting of the spectral profiles. A portion from the spectral series recorded by Jin and Ikawa [6] for two isotherms 650 and 673 K has been chosen for the fitting. Typical spectra are shown in Fig. 4. The quality of a fit can easily be improved provided one would assume more than three vibrational bands in expense of an increased number of adjustable parameters. Neither the overall shape nor the dimer fraction change substantially, however, given the number of bands is doubled. We believe that detailed representation of the overtone dimer spectrum is presently beyond the limits of reliability of our concept. That is why we restricted ourselves by the simplified modeling which operates with only three effective dimer bands. On the average the quality of a fit is quite satisfactory. Here again, the fitting at highest density is as good as at much lower density in spite of our belief that the assumption of binary mixture is no longer valid in steam as dense as 0.04 g cm^{-3}. Fig. 3 shows the isothermal pressure variations of the monomer mass fraction. Surprisingly, at least at $T=673$ K, these fractions retrieved either from the spectra of the fundamental or from the overtone are in good agreement with each other. The equilibrium constants are summarized in Table 4.

5. Comparison with literature data

Interestingly, the half-widths of (effective) dimer bands in the overtone display notable regularity (see Fig. 5) with respect to pressure exhibiting no pronounced temperature trend. The retrieved dimer intensities keep reasonably constant as a function of pressure and neither exhibit strong temperature variations. Strong absorption band at

Table 5
Measured and calculated OH-overtone frequencies (cm^{-1}) and relative intensities[a] of $(H_2O)_2$

Symmetry	Mode	Ne matrix [5]		Schofield et al. [2]		This work[b]	
		ν	I	ν	I	ν	I
A'	$2\nu_1$ (PA)	7206.6	0.18	7200	0.29	7203	0.22
A''	$\nu_1+\nu_3$ (PA)	7245	–	7239	1.3	7239	0.89
A'	$2\nu_3$ (PA)	–	–	7440	0.004	7430	0.04
A'	$2\nu_1$ (PD)	7018	0.19	7047	0.005	7059	0.0017
A''	$\nu_1+\nu_3$ (PD)[c]	7237.1	0.86	7238	0.79	7229.5	0.59
A'	$2\nu_3$ (PD)[c]	7362	0.09	7371	0.08	7377	0.1

[a] The relative intensities are scaled to a ν_1 (PD) intensity of 100 appropriate to each individual intensity data set.
[b] Vibrational frequencies are obtained using potential parameteres listed in Table 1. Intensities are calculated using ab initio dipole parameters as described in Sect 2.
[c] The assignment of $2\nu_3$ (PD) and $\nu_1+\nu_3$ (PD) vibrations follows that from [5]. Note, that in case of Schofield et al. data this assignment differs from that in original publication [2].

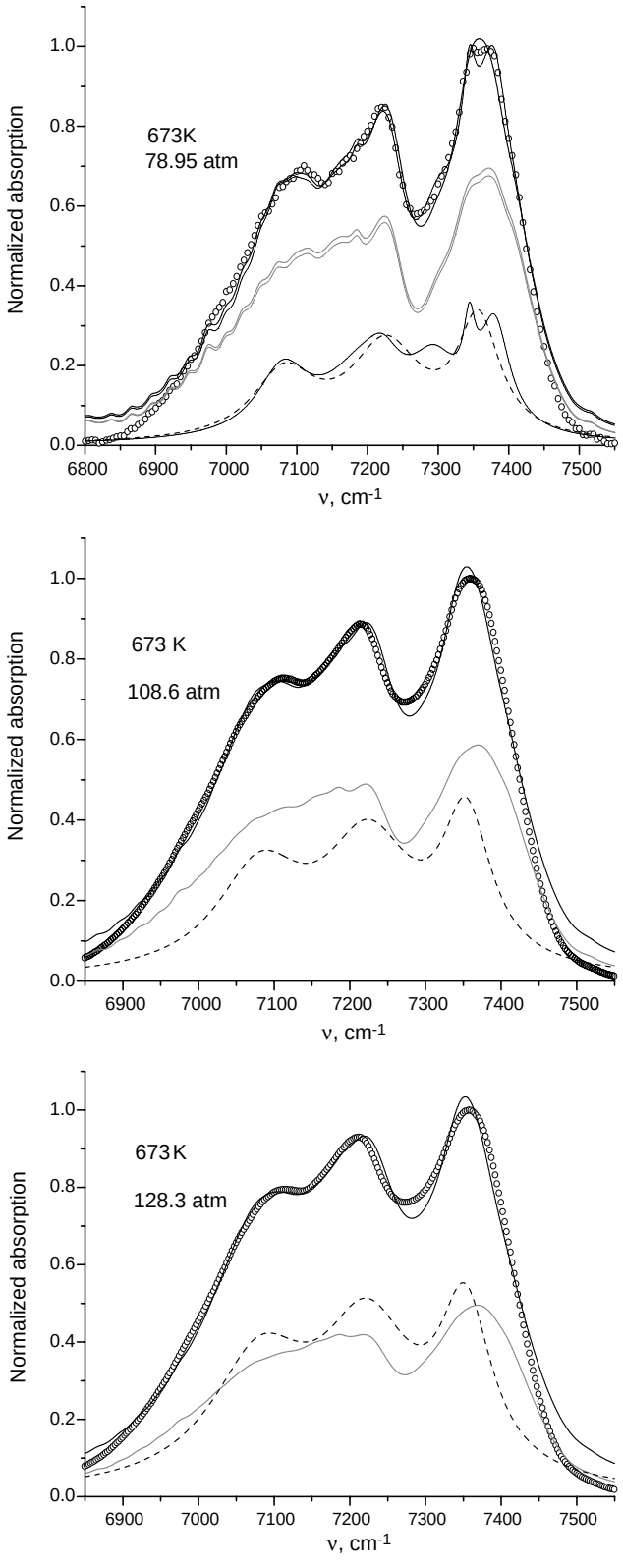

Fig. 4. Water vapor absorption in the OH stretching overtone. Not all experimental points from [6] are displayed for the sake of clarity. Light, dash, and solid traces refer to the monomer, dimer, and resulting spectra, respectively. Lighter repetitions of each of these traces in the uppermost panel of this figure show the variant of a fit assuming six adjustable dimer bands instead of three.

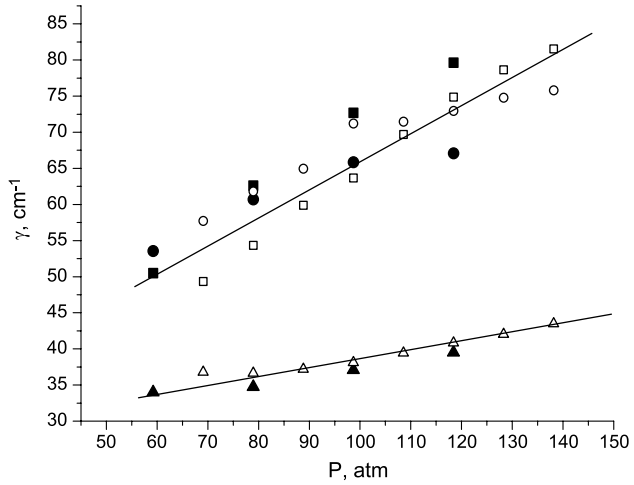

Fig. 5. Pressure variations of the effective partial dimer bandwidths in the OH overtone. Solid and empty marks refer to 650 and 673 K isothermal spectral series, respectively. Circles and squares stand for two lower frequency components among three (effective) dimer bands, triangles relate to the high frequency component.

7230 cm^{-1} is roughly equal in intensity to the doubled overtone intensity in a monomer. Two weaker satellites are clearly seen in Fig. 6, the intensity of which is by no means negligible with respect to the central peak. This result is in obvious contradiction with either the observations in the matrices or with ab initio predictions. Fig. 6 shows that quantum chemical based calculations result in absorption intensity beyond the central peak which is indeed significantly lower than that retrieved from the spectral fit. The data taken in Ne matrix [5] also evidence in favor of significantly lower intensity of satellites off the central peak.

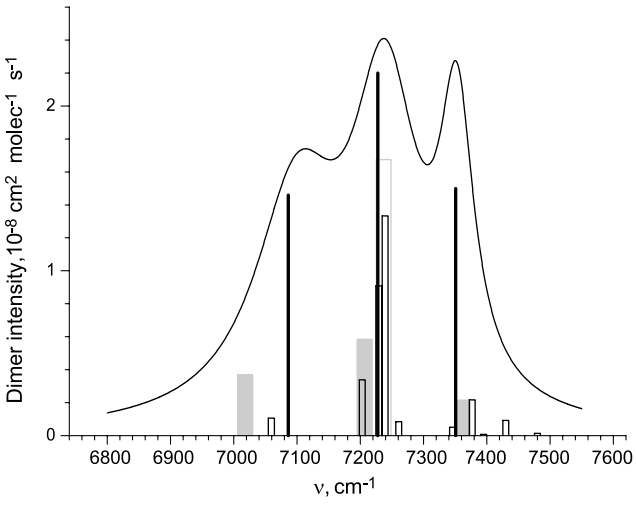

Fig. 6. Partial dimer bands in the OH stretching overtone. Solid sticks stand for the dimer bands obtained from the spectral fit in the present work. Solid line shows typical dimer profile from this fit. Empty and shaded rectangles stand, respectively, for ab initio based anharmonic calculations from the present work and for the data reported in [5] for the water dimers trapped in Ne matrix.

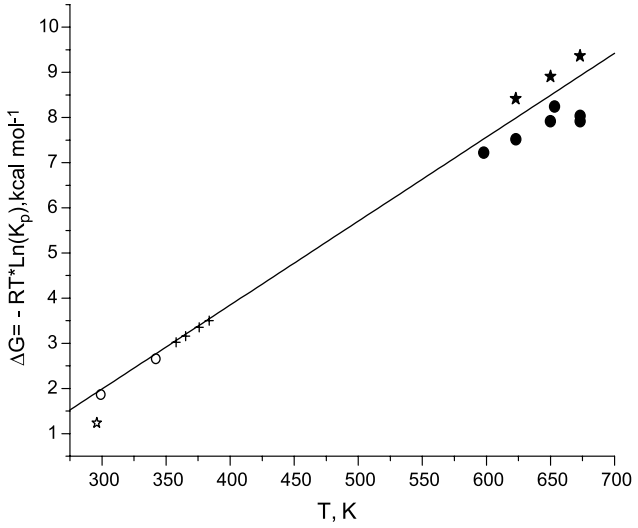

Fig. 7. Gibbs free energy of dimerization as a function of temperature. Solid circles come from the present work. Solid asterisks, empty circles and empty asterisk are from Refs [6,13,24], respectively. The crosses refer to the equilibrium constant from Ref. [8], the straight line is plotted for the sake of clarity.

The integrated dimer intensity obtained from our fit is on the order of 8-12 km mol^{-1} that is the estimated molar intensity in a dimer is likely to exceed that in a monomer. This conclusion disagrees both with ab initio and Ne matrix results and points out presumably at the model drawback. It has to be realized, however, that ab initio based calculations of the overtone intensity are not as precise as the calculations in the fundamental range. From the other hand, our adopted simplified dimer bandshape modeling also precludes accurate estimate for the dimer overtone intensities because of a number of simplifications which have been made. Moreover, even the monomer overtone intensity looks a matter of controversy. Jin and Ikawa [6] estimated it as 4.5 km mol^{-1} from the extrapolation of the linear plot of molar absorption intensity versus pressure to zero vapor pressure. This figure differs significantly from the HITRAN value (4.0 km mol^{-1}) quoted above. The problem of the monomer or dimer intensities in the OH stretching overtone range is worth then of forthcoming study in detail.

Fig. 7 shows temperature variations of the Gibbs free energy in reaction of the water dimer formation. It is seen that the values obtained in the present work are in quite good agreement with independent estimates reported previously in the literature.

6. Conclusions

This work provides further evidences for the important role played by molecular aggregation in pressurized steam. Following previous publications (see [6,7,9,10] and references therein) we explored the idea of the dominant contribution from the water dimers formation to the observed density variations in absorption bandshape profiles both in the OH fundamental and overtone. Our spectral simulation was essentially supported by ab initio calculations of the water dimer molecular characteristics accompanied by the variational solution of vibrational problem in advanced account for anharmonicity. Good agreement is obtained between the dimer fractional abundance retrieved at selected temperature from the spectra taken in the OH fundamental and overtone. The estimated Gibbs free energy for dimerization is in accord with independent data. The conclusion was drawn on the failure of assumption of the monomer–dimer mixture at densities exceeding roughly 0.04 g cm^{-3}. Discrepancies in the estimates for the monomer and the dimer integrated intensity of absorption in the region of the OH stretching overtone were found. Detailed reconsideration of the monomer and dimer absorption in the overtone range is thus worth of doing. To make our spectral model reliable the contribution from non-additivity effects to the monomer rovibrational absorption profile would be desirable to account for. The opportunity seems promising to isolate dimer contributions to the spectral bandshapes from those of larger oligomers in order to better characterize the individual spectral signatures of small water aggregates.

Acknowledgements

A.A.V. and A.I.P. acknowledge partial support from RFBR Grants 02-05-64529 and 02-03-32416.

References

[1] G.R. Low, H.G. Kjaergaard, J. Chem. Phys. 110 (1999) 9104.
[2] D.P. Schofield, H.G. Kjaergaard, Phys. Chem. Chem. Phys. 5 (2003) 3100.
[3] J.P. Perchard, Chem. Phys. 266 (2001) 109.
[4] J.P. Perchard, Chem. Phys. 273 (2001) 217.
[5] Y. Bouteiller, J.P. Perchard, Chem. Phys. 305 (2004) 1.
[6] Y. Jin, S. Ikawa, J. Chem. Phys. 119 (2003) 12432.
[7] G.V. Bondarenko, Y.E. Gorbaty, Mol. Phys. 74 (1991) 639.
[8] L.A. Curtiss, D.J. Frurip, M. Blander, J. Chem. Phys. 71 (1979) 2703.
[9] A.A. Vetrov, PhD Thesis, Institute for High Temperatures, USSR Academy of Sciences, Moscow, 1976 [in Russian].
[10] M.A. Styrikovich, G.V. Yukhnevich, O.I. Kondratov, A.A. Vetrov, A.A. Vigasin, Proceedings of eighth International Conference on Properties Water and Steam, Giens, 1974, p. 1000.
[11] F. Huisken, in: A.A. Vigasin, Z. Slanina (Eds.), Molecular Complexes in Earth's, Planetary, Cometary, and Interstellar Atmospheres, World Scientific, Singapore, 1998, p. 238.
[12] K. Pfeilsticker, A. Lotter, C. Peters, H. Bösch, Science 300 (2003) 2078.
[13] I.V. Ptashnik, K.M. Smith, K.P. Shine, D.A. Newnham, Quart. J. Roy. Meteorol. Soc. 130 (2004) 2391.

[14] L.A. Gribov, A.I. Pavlyuchko, Variational Methods for Solving Anharmonic Problems in the Theory of Vibrational Spectra of Molecules, Nauka, Moscow, 1998. [in Russian].
[15] M.W. Schmidt, K.K. Baldridge, J.A. Boatz, S.T. Elbert, M.S. Gordon, J.H. Jensen, S. Koseki, N. Matsunaga, K.A. Nguyen, S.J. Su, T.L. Windus, M. Dupuis, J.A. Montgomery, J. Comput. Chem. 14 (1993) 1347.
[16] L.S. Rothman, R.R. Gamache, R.H. Tipping, C.P. Rinsland, M.A.H. Smith, D.C. Benner, V.M. Devi, J.-M. Flaud, C. Camy-Peyret, A. Perrin, A. Goldman, S.T. Massie, L.R. Brown, J. Quant. Spectrosc. Radiat. Transfer 48 (1992) 469.
[17] D.J. Swanton, G.B. Backskay, N.S. Hush, Chem. Phys. 82 (1983) 303.
[18] S. Chin, T.A. Ford, W.B. Person, J. Mol. Struct. 113 (1984) 341.
[19] B.A. Zilles, W.B. Person, J. Chem. Phys. 79 (1983) 65.
[20] E.W. Lemmon, M.O. McLinden, D.G. Friend, in: P.J. Linstrom, W.G. Mallard (Eds.), NIST Chemistry WebBook, NIST Standard Reference Database 69, National Institute of Standards and Technology, Gaithersburg, MD, 2001 (http://webbook.nist.gov).
[21] A.A. Vigasin, in: C. Camy-Peyret, A.A. Vigasin (Eds.), Weakly Interacting Molecular Pairs: Unconventional Absorbers of Radiation in the Atmosphere NATO ARW Proceedings Series, Kluwer Academic Publisher, 2003, p. 23.
[22] Q. Zou, P. Varanasi, J. Quant. Spectrosc. Radiat. Transfer 82 (2003) 45.
[23] F. Huisken, M. Kaloudis, A.A. Vigasin, Chem. Phys. Lett. 269 (1997) 235.
[24] N. Goldman, R.S. Fellers, C. Leforestier, R.J. Saykally, J. Phys. Chem. 105 (2001) 515.